the magma that produced the Montana diatremes closely resembled magmas known to be parental to kimberlite in diatremes in Arkansas, Africa, Siberia, and elsewhere. Although inclusions of eclogite and garnet peridotite that are typical of most kimberlites are lacking in most Montana diatremes, some inclusions in these diatremes may derive from the lower crust or the upper mantle.

Despite recent allegations that kimberlite and its crystalline inclusions have rather shallow origins (*21*), the evidence provided by the inclusions argues for a deep, probably mantle, origin of the material now observed as kimberlite and of the associated alkalic ultramafic magmas; the evidence implies a substantial source of calcium, sodium, potassium, and gas (partly carbon dioxide) in the mantle.

B. CARTER HEARN, JR.
*U.S. Geological Survey,
Washington, D.C. 20242*

References and Notes

1. Considerable controversy has long been associated with the definition and origin of kimberlite. Kimberlite is a mixture of the end products of several processes of fragmentation and alteration, all of which tend to obscure the parental role of alkalic ultramafic magmas in the genesis of many but not all kimberlites. The generally accepted and descriptively useful definition of kimberlite is a brecciated, altered rock of porphyritic appearance, rich in altered olivine, rich in inclusions of wall rocks, and rich in deep-seated xenoliths and xenocrysts (characteristically pyropic garnet, chromian diopside, and magnesian ilmenite).
2. B. F. Buie, in *Geol. Soc. Amer. Bull. 52* (1941), pp. 1799–1805 [Buie mentioned another ultramafic occurrence (queried in fig. 1) not specifically located on the map by E. S. Larsen (pl. 1)].
3. F. Reeves, in *U.S. Geol. Surv. Bull. 751-C* (1924), pl. 13, pp. 96–7 (totals include one diatreme and one dike outlined but not colored in pl. 13).
4. M. M. Knechtel, *U.S. Geol. Surv. Oil Gas Invest. Prelim. Map 4* (1944); in *U.S. Geol. Surv. Bull. 1072-N* (1959), pl. 52.
5. Mica peridotites are a broad group of alkalic ultramafic rocks that are rich in olivine (commonly of two compositions) and mica (commonly phlogopite), with varying amounts of melilite, nepheline, pyroxene, apatite, and perovskite. Monticellite peridotite and alnoite can be considered varieties of mica peridotite.
6. Monticellite peridotite is a forsterite-monticellite-nepheline-phlogopite rock. Alnoite is a forsterite-melilite-nepheline-phlogopite rock; it was originally defined as an olivine-clinopyroxene-melilite-biotite-nepheline rock, but the term has been used by many workers, including Buie, for alkalic ultramafic rocks bearing melilite and free of pyroxene. Such rocks, containing from 32 to about 40 percent silica, are among the least-silicic igneous rocks known.
7. Relative age determined by detailed mapping by me.
8. E. S. Larsen, in *Geol. Soc. Amer. Bull. 51* (1940), p. 891; in *Geo. Soc. Amer. Bull. 52* (1941), p. 1862. An alnoite from a sill west of Winnett in central Montana was described in detail by C. S. Ross, *Amer. J. Sci.* **11**, 218 (1926); that sill is part of a group of alkalic ultramafic occurrences geographically separate from the Missouri Breaks diatremes.
9. L. V. Pirsson, *Amer. J. Sci.* **20**, 35 (1905); E. S. Larsen, in *Geol. Soc. Amer. Bull. 51* (1940), p. 887.
10. B. C. Hearn, Jr., W. T. Pecora, W C Swadley, in *U.S. Geol. Surv. Bull. 1181-B* (1964), pp. 20–7. Lithologic characteristics of most of the sandstones of the Wasatch and Fort Union formations are so distinctive that the rocks can be identified even when they occur as 2.5-cm inclusions.
11. A Bearpaw Mountains source is clearly shown in one diatreme by rounded pebbles of igneous rocks closely resembling some of the youngest dikes, dated as middle Eocene or possibly late Eocene in age, in Bearpaw Mountains.
12. F. Reeves, in *U.S. Geol. Surv. Bull. 751-C* (1924), p. 71; in *Geol. Soc. Amer. Bull. 57* (1946), p. 1033. Reeves's mapping of these structures provided the basis for his hypothesis of gravitational sliding of the volcanic rocks and their floor in the vicinity of Bearpaw Mountains.
13. Similar pelletal fragments of igneous rock in ultramafic diatremes elsewhere have been described and illustrated by G. W. Rust, *J. Geol.* **45**, 60, figs. 8–14 (1937); and H. Cloos, *Geol. Rundschau* **32**, 716, fig. 10 (1941).
14. J. F. Lovering and A. J. R. White, *J. Petrology* **5**, 195 (1964).
15. P. A. Wagner, *The Diamond Fields of Southern Africa* (Transvaal *Leader*, Johannesburg, 1914), pp. 19–23, 49–50; A. F. Williams, *The Genesis of the Diamond* (E. Benn, London, 1932), pp. 258–62, 274–5, 291–2, 298; G. W. Rust, *J. Geol.* **45**, 56 (1937); H. Cloos, *Geol. Rundschau* **32**, 709 (1941); V. S. Sobolev, *Pacific Sci.* **17**, 453 (1963); J. Chronic, M. E. McCallum, C. S. Ferris, in *Geol. Soc. Amer. Spec. Paper 87* (1966), p. 280.
16. E. M. Shoemaker, in *Physics and Astronomy of the Moon*, Z. Kopal, Ed. (Academic Press, New York, 1962), pp. 283–359; in *Petrologic Studies: A Volume to Honor A. F. Buddington*, A. E. J. Engel, H. L. James, B. F. Leonard, Eds. (Geol. Soc. Amer., 1962), pp. 327–55.
17. A less-likely alternative is that some slices could be remnants of a cylindrical volume of rock that subsided during the initial formation of the diatreme and that has since been cored out by further subsidence or eruption. Emplacement of the slices by descent in an open ring fracture is unlikely in view of the distances involved, the considerable evidence of lateral compression in the pipes, and the probability that the pipes narrow with depth.
18. A. R. McBirney, *Amer. J. Sci.* **257**, 431 (1959).
19. Meimechite is an ultrabasic rock rich in olivine (usually altered) in a sepentine-rich groundmass; it has been called the extrusive equivalent of kimberlite by Russian geologists.
20. P. A. Wagner, in *Handbuch der Regionalen Geologie*, vol. 7, pt. 7a, *The Union of South Africa*, G. Steinmann and O. Wilckens, Eds. (Winters Universitatsbuchhandlung, Heidelberg, Germany, 1929), p. 152.
21. C. F. Davidson, *Econ. Geol.* **59**, 1368 (1964); **60**, 1735 (1965); **61**, 786 (1966).
22. C. P. Ross, D. A. Andrews, I. J. Witkind, U.S. Geol. Surv., 1955.
23. I thank C. P. Sabine, N. L. Hickling, J. M. Garihan, J. J. Papike, and H. R. Shaw (U.S. Geological Survey) for assistance and stimulating discussion; and D. R. Seely, P. H. Masson, and J. G. Bond (Jersey Production Research Co., Tulsa, Okla.) for calling my attention to an occurrence of pyroclastic rocks. Publication authorized by the director, U.S. Geological Survey.

27 December 1967

Lunar Gravity: Preliminary Estimates from Lunar Orbiter

Abstract. *Tracking data from the lunar orbiters have been analyzed for information regarding Moon's gravity field. These preliminary results include values of a set of harmonic coefficients through degree 4 in the tesserals and degree 8 in the zonals. Implications regarding Moon's mass distribution are discussed: one implication is that Moon is nearly homogeneous.*

Lunar Orbiter V, launched 1 August 1967, culminated NASA's Lunar Orbiter Program under which four Lunar Orbiters already had been successful. Although the prime mission for these orbiters is photographic, analysis of the Doppler tracking data is providing gravity-field information for the selenodesy experiment.

We are intensively analyzing the tracking data (*1*) in order to map Moon's gravity field and for any other information. Similar work with the same data is being performed elsewhere, but on an immediate, short-term basis; our work is a continuing long-term effort to refine the results. It is hoped that some of the first results will (i) resolve the long-standing question of whether or not the density increases toward the center of Moon, and (ii) establish the degree of north-south asymmetry. These two questions should be answered when numerical values of the 2nd- and 3rd-degree zonal harmonics C_{20} and C_{30} are obtained. We now present some preliminary results that include values for these two harmonics; we emphasize that these results are preliminary and subject to revision as the work of analysis proceeds.

The lunar gravity field is described, in terms of its potential Φ through harmonic coefficients C_{nm} and S_{nm}, by the formula

$$\Phi = \frac{\mu}{r}\left[1 + \sum_{n=2}^{\infty}\sum_{m=0}^{n}\left(\frac{R}{r}\right)^{m} P_n{}^m(\sin\phi)\,(C_{nm}\cos m\lambda + S_{nm}\sin m\lambda)\right]$$

in which μ is the gravity constant, whose value is taken from Mariner IV estimates as 4902.78 km^3/sec^2; R is the mean radius of Moon, whose value is not critical for these computations, but which is taken as 1738.09 km; $P_n{}^m(z)$ is the associated Legendre poly-

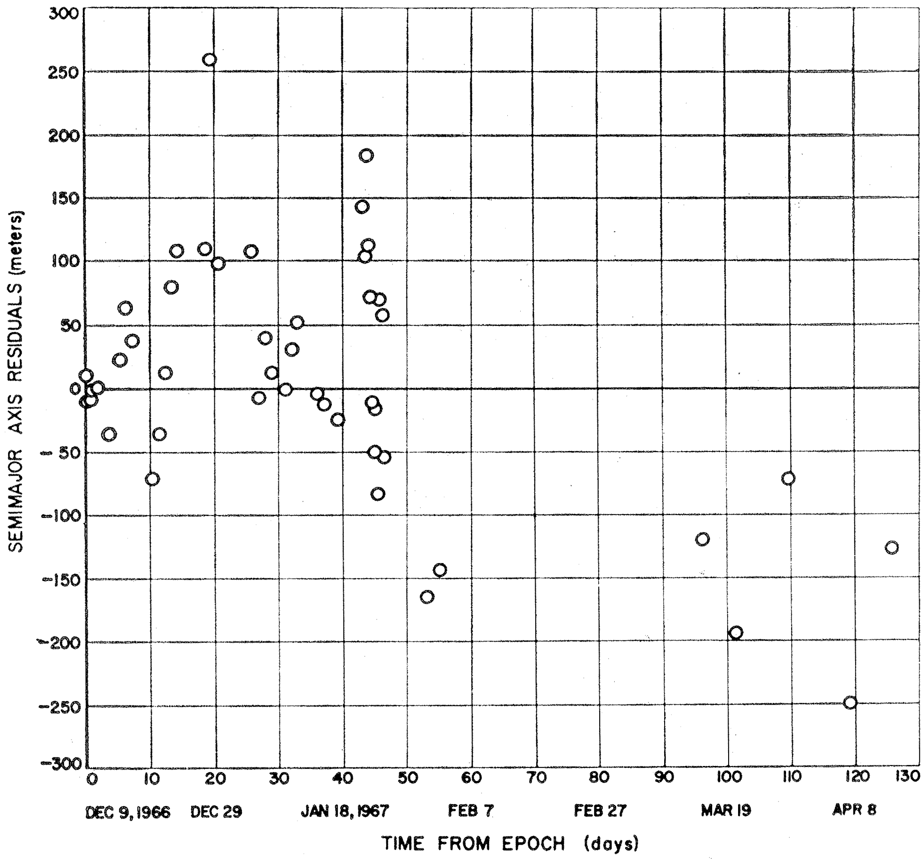

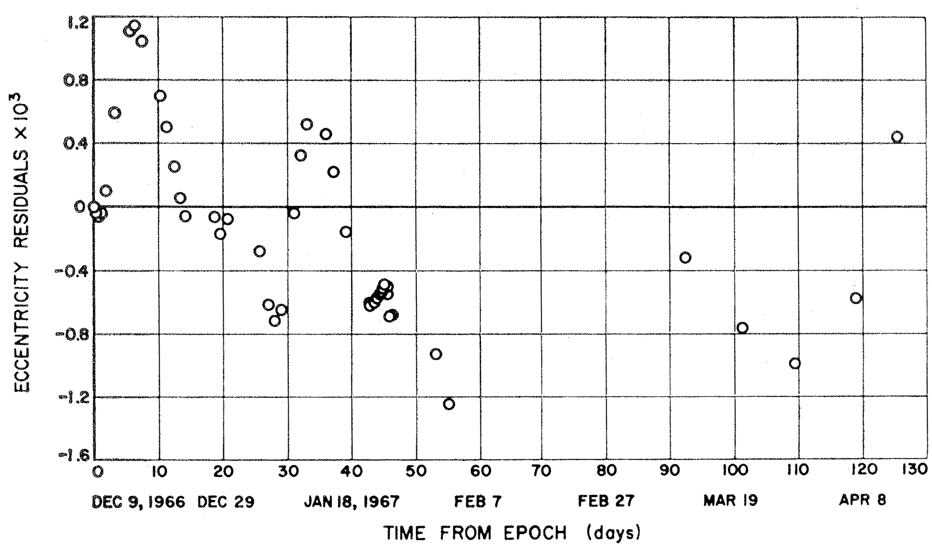

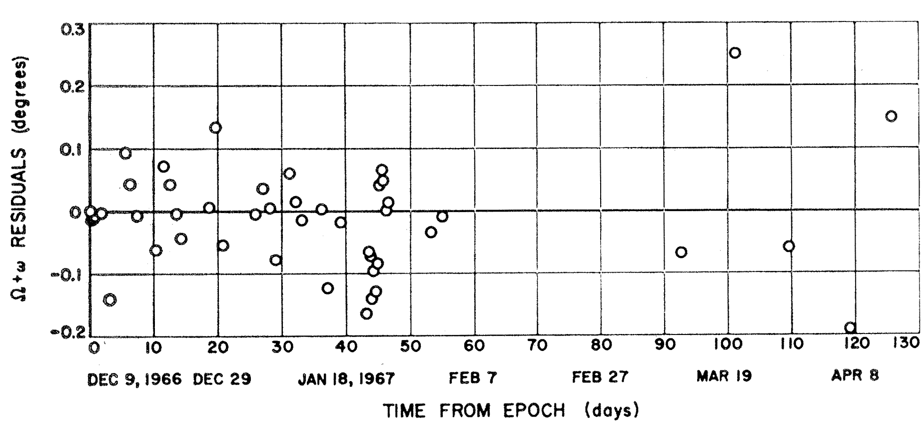

Fig. 1 (top left). Semimajor axis residuals (meters).

Fig. 2 (center left). Eccentricity residuals $\times 10^3$.

Fig. 3 (bottom left). $\Omega + \omega$ Residuals (degrees.

nomial in z: and r, ϕ, and λ are spherical polar coordinates.

Thus Φ is determined when numerical values are assigned to C_{nm} and S_{nm}. We chose to limit the number of terms in the series for Φ by considering only those up to and including 4th degree and 4th order ($n = m = 4$), plus C_{50}, C_{60}, C_{70}, and C_{80}; that is, 25 harmonics in all.

In Table 1 are the coefficient values, and their standard deviations, as obtained from the data from the first four orbiters. Represented here are orbits of 12-, 18-, 21-, and 85-degree inclination, and of 2766-, 3752-, and 6148-km semimajor axes (in various combinations). Six separate arcs were used, the longest of which was 125 days. To show the goodness of fit we include graphs of residuals (corresponding to the longest arc from Lunar Orbiter II used in the analysis) of semimajor axis, eccentricity, and node (Ω) plus argument of pericenter (ω) in Figs. 1 to 3, respectively. The raw Doppler data from the NASA Deep Space Network (*2*) are extremely precise (noise level, 1 mm/sec); however, for sampling the lunar environment, the data are rather skimpy. Additional data from orbits with inclinations between 21 and 85 degrees would add considerable strength to the determinations. We feel that the statistics, in particular our standard deviations, are meaningful numbers and reflect the adequacy of the data for estimation of the harmonics. To be specific we chose a weighting factor of 7000 mm/sec for the Doppler residuals, a factor many times greater than the 1-mm/sec noise level, in order to be consistent with the scatter in the Kepler element residuals as shown in Figs. 1 to 3.

The values of C_{20} and C_{22}, derived from Earth-based observations, serve as a reference against which one may judge the adequacy of Table 1 numbers. Jeffreys (*4*) suggests values, of the moment-of-inertia ratios, corresponding to

$$C_{20} = (-2.093 \pm 0.020) \times 10^{-4}$$

and

$$C_{22} = (0.210 \pm 0.004) \times 10^{-4}$$

for a homogeneous Moon. He also deduces, from geophysical arguments, that Moon is slightly denser toward the center—sufficiently so to reduce these values by about 1 percent. He bases his numbers on lunar libration theory rather than on lunar orbit theory which in its present state requires much greater value (in absolute magnitude) of C_{20}, corresponding to a Moon with crust denser than interior (*5*). The value of C_{20} obtained by us from Lunar Orbiter data is some 3 percent less in magnitude than the homogeneous-Moon value and thus corresponds to a Moon having an interior density moderately higher than crust density. Tolson and Gapcynski (*6*, *7*) and Michael *et al.* (*7*) derive somewhat different results from some preliminary reductions of these data—although an almost homogenous Moon is implied, as we infer. (Michael *et al.* used a direct fit to the raw data, whereas we used the method of averages for the reduction.) Thus more data must be analyzed before consistent solutions are obtained.

For the odd zonals, we have no nonorbiter values for comparison. These coefficients describe the north-south asymmetry, sometimes referred to as the pear-shape. Akim (*8*) has published a value of C_{30}, based on a Russian orbiter, equal to -0.363×10^{-4}, which is somewhat larger numerically than ours, but of the same sign.

Table 2 lists the pairs of coefficients having high correlations. Of course the values of the correlations are completely dependent on the types of orbits from which the data were taken; a more complete set of orbits would yield data giving smaller correlations.

We must emphasize that these results are preliminary; the data are still being refined and, we hope, will submit to better fits. Furthermore, more data should soon become available from Lunar Orbiter V.

J. LORELL
W. L. SJOGREN
Systems Analysis Research Section, Systems Division, Jet Propulsion Laboratory, California Institute of Technology, Pasadena

Table 1. Preliminary estimates of lunar-gravity harmonics, based on Lunar Orbiters I–IV. Normalization factor:

$$\{[(n-m)!/(n+m)!](2n+1)\ (2-\delta_0^{\,m})\}^{\frac{1}{2}}$$

Harmonic coefficient	Coefficient values (× 10⁴) Not normalized	Coefficient values (× 10⁴) Normalized	S.D. ($\sigma \times 10^4$) Not normalized	S.D. ($\sigma \times 10^4$) Normalized
C_{20}	−2.0263	−0.9062	0.0143	0.0064
C_{21}	−0.0878	− .0680	.0131	.0101
C_{22}	0.2191	0.3394	.0249	.0386
C_{30}	−0.2223	−0.0840	.0262	.0100
C_{31}	0.3636	0.3366	.0025	.0023
C_{32}	−0.0257	−0.0752	.0058	.0170
C_{33}	− .0265	− .1900	.0079	.0567
C_{40}	0.0941	0.0314	.0190	.0063
C_{41}	−0.1236	−0.1303	.0046	.0049
C_{42}	0.0361	0.1614	.0034	.0152
C_{43}	.0164	.2747	.0021	.0351
C_{44}	.0091	.4313	.0011	.0521
C_{50}	−0.1614	−0.0487	.0321	.0097
C_{60}	− .1089	− .0302	.0121	.0034
C_{70}	0.1734	0.0448	.0122	.0031
C_{80}	−0.2011	−0.0488	.0114	.0028
S_{21}	0.0150	0.0116	.0139	.0108
S_{22}	.1310	.2029	.0335	.0519
S_{31}	.0740	.0685	.0032	.0029
S_{32}	−0.0200	−0.0586	.0063	.0184
S_{33}	− .0496	− .3557	.0114	.0818
S_{41}	0.0564	0.0595	.0051	.0054
S_{42}	.0051	.0228	.0035	.0157
S_{43}	−0.0276	−0.4618	.0015	.0251
S_{44}	0.0079	0.3739	.0011	.0521

Table 2. Pairs of coefficients with correlations greater than 0.8.

Pair	Correlation
C_{20} and C_{40}	+.94
C_{20} and C_{60}	+.82
S_{21} and S_{41}	+.81
C_{30} and C_{50}	+.97
S_{32} and C_{42}	−.91
C_{32} and S_{42}	+.87
S_{33} and C_{43}	−.86
C_{40} and C_{60}	+.84
C_{50} and C_{70}	+.86

References and Notes

1. J. Lorell, W. L. Martin, W. L. Sjogren, *Space Programs Summary 37-43* (Jet Propulsion Lab., Pasadena, Calif., 1967), vol. 4.
2. J. Lorell, J. D. Anderson, W. L. Sjogren, "Characteristics and format of the tracking data to be obtained by the NASA deep space instrumentation facility for Lunar Orbiter," *TM 33-230* (Jet Propulsion Laboratory, Pasadena, Calif., 1965).
3. J. Lorell, W. L. Sjogren, D. Boggs, "Compressed tracking data used for first iteration in selenodesy experiment, Lunar Orbiter I and II," *TM 33-343* (Jet Propulsion Lab., Pasadena, Calif., 1967).
4. H. Jeffreys, *Proc. Roy. Soc. London Ser. A* **296**, 245 (1967).
5. W. J. Eckert, *Astron. J.* **70**, 787 (1965).
6. R. H. Tolson and J. P. Gapcynski, "An analysis of the lunar gravitational field as obtained from Lunar Orbiter tracking data," paper presented before IQSY/COSPAR Assemblies, London, 17–28 July 1967.
7. W. H. Michael, Jr., R. H. Tolson, J. P. Gapcynski, "Preliminary results on the gravitational field of the moon from analysis of Lunar Orbiter tracking data," paper presented before American Geophysical Union Annual Meeting, Washington, D.C., 17 April 1967.
8. E. L. Akim, *Dokl. Akad. Nauk SSSR* **170**(4), 799 (1966).
9. Work performed by the Jet Propulsion Laboratory, California Institute of Technology, Pasadena, and sponsored by NASA under contract NAS 7-100.

5 October 1967

Crescentic Landforms along the Atlantic Coast of the United States

Abstract. *An uninterrupted series of hierarchically arranged crescentic coastal landforms occurs along the Atlantic coast. Dimensional analysis suggests a geometric relation between order, amplitude, and number. The processes responsible for these features also may be continuous in nature.*

Crescent-shaped sand ridges with their concave sides facing the sea are among the most frequently observed landforms in coastal areas composed of sedimentary materials. Among the smallest of these forms is the beach cusplet, measuring about 1.5 m between tips of the crescent. Even the casual visitor is familiar with these swash-zone features (Fig. 1a) and is aware that their life-spans are short: usually they appear and disappear with the turn of the tide. More common are the larger, typical beach cusps which range from about 8 to 25 m from apex to apex (Fig. 1b); they usually develop by erosion of the seaward faces of depositional beach ridges during fair weather, and have life-spans measurable in days. Still-larger crescentic forms are relatively common, including Evans's (*1*) "storm cusps," which measure from 70 to 120 m and develop during periods of relatively heavy seas. Shepard's (*2*) "giant cusps," also known as shoreline rhythms or migrating sand waves (*3*), range in size from 700 to 1500 m and appear to be characteristic of areas or times of relatively strong littoral currents (Fig. 1c).

During investigations of shoreline processes along the coast of North Carolina, two attributes of these cuspate features were observed: (i) they seem to be hierarchically arranged—smaller features are grouped within larger ones; and (ii) a tendency toward clustering by size; Fig. 2 shows the size-frequency distribution of about 750 cuspate features along the Outer Banks of North Carolina and the central Atlantic coast. The modes on this curve (Fig. 2) confirm the distinct hierarchical nature of these features, as well as logarithmic spacing between groups. These data are recast in Fig. 3, in which modal values for each group (called orders) are plotted as single points, and a line connecting these points is extended to cuspate forms of larger size.